Estimation of Pulmonary Motion in Healthy Subjects and Patients with Intrathoracic Tumors Using 3D-Dynamic MRI: Initial Results

Christian Plathow, MD, MSc[1, 3]
Max Schoebinger, MSc[2]
Felix Herth, MD[4]
Siegfried Tuengerthal, MD[5]
Heinz-Peter Meinzer, MSc[2]
Hans-Ulrich Kauczor, MD[6]

Index terms:
Dynamic MRI
Intraparenchymal lung motion
Biomechanics
Tumor
Pleural mesothelioma

DOI:10.3348/kjr.2009.10.6.559

Korean J Radiol 2009;10:559-567
Received March 30, 2009; accepted after revision June 23, 2009.

[1]Department of Radiology, [2]Department of Medical and Biological Informatics, German Cancer Research Center Heidelberg, Germany; [3]Department of Nuclear Medicine, University of Freiburg, Germany; [4]Department of Internal Medicine, [5]Department of Diagnostic Radiology, Clinic of Thoracic Disease, Germany; [6]Department of Diagnostic and Interventional Radiology, University of Heidelberg, Germany

Address reprint requests to:
Christian Plathow, MD, Department of Nuclear Medicine, University of Freiburg, Hugstetter 55, 76109 Freiburg, Germany.
Tel. ++49-761-2707421
Fax. ++49-761-2703989
e-mail: christian.plathow@uniklinik-freiburg.de

Objective: To estimate a new technique for quantifying regional lung motion using 3D-MRI in healthy volunteers and to apply the technique in patients with intra- or extrapulmonary tumors.

Materials and Methods: Intraparenchymal lung motion during a whole breathing cycle was quantified in 30 healthy volunteers using 3D-dynamic MRI (FLASH [fast low angle shot] 3D, TRICKS [time-resolved interpolated contrast kinetics]). Qualitative and quantitative vector color maps and cumulative histograms were performed using an introduced semiautomatic algorithm. An analysis of lung motion was performed and correlated with an established 2D-MRI technique for verification. As a proof of concept, the technique was applied in five patients with non-small cell lung cancer (NSCLC) and 5 patients with malignant pleural mesothelioma (MPM).

Results: The correlation between intraparenchymal lung motion of the basal lung parts and the 2D-MRI technique was significant ($r = 0.89$, $p < 0.05$). Also, the vector color maps quantitatively illustrated regional lung motion in all healthy volunteers. No differences were observed between both hemithoraces, which was verified by cumulative histograms. The patients with NSCLC showed a local lack of lung motion in the area of the tumor. In the patients with MPM, there was global diminished motion of the tumor bearing hemithorax, which improved siginificantly after chemotherapy (CHT) (assessed by the 2D- and 3D-techniques) ($p < 0.01$). Using global spirometry, an improvement could also be shown (vital capacity 2.9 $\pm$ 0.5 versus 3.4 L $\pm$ 0.6, FEV1 0.9 $\pm$ 0.2 versus 1.4 $\pm$ 0.2 L) after CHT, but this improvement was not significant.

Conclusion: A 3D-dynamic MRI is able to quantify intraparenchymal lung motion. Local and global parenchymal pathologies can be precisely located and might be a new tool used to quantify even slight changes in lung motion (e.g. in therapy monitoring, follow-up studies or even benign lung diseases).

In many pulmonary pathology cases, the compliance of lung tissue increases locally or globally, leading to clinical symptoms such as dyspnea in the end (1, 2). A key aspect of pulmonary physiology that can be measured using MRI is lung motion. Surrogate measures based on the motion of the chest wall and diaphragm have been reported (3–5); and, can be compared to conventional pulmonary function tests such as spirometric local information of, for example, the hemithorax.

Grid-tagging techniques allow for the direct assessment of regional motion and local mechanical properties of moving structures in the human body (6, 7). However, there are limitations due to the relatively low spatial resolution of the estimated motion

fields, stemming from the coarse grid intervals that are currently practicable. Another problem is the fading of the grid due to the T1 decay time of the tissue and the difficulty of applying the method in 3D. In addition, 3D-imaging techniques covering a whole volume and not just a certain aspect or dimension as in 2D-imaging techniques might be the technique of choice, which, so far are frequently suffering from a lack of sufficient temporal resolution (8). Thus 3D techniques are still the focus of scientific research (8, 9).

Recently, a new approach has been proposed using a dense motion field as a potential indirect parameter of lung compliance (10, 11). Using MRI, this technique was introduced in a small group of healthy subjects with limited temporal resolution. Using a similar technique, it could be shown that the motion of pulmonary nodules during the breathing cycle can be quantified (9). A 3D-quantification of the motion of the lung parenchyma during the breathing cycle has not been quantified or visualized so far.

In this study we propose a technique using dynamic 3D-MRI sequences with high temporal resolution and a new semiautomatic post-processing tool to quantify intraparenchymal lung motion. For verification the 3D-imaging technique was correlated with an established 2D-technique; this approach has been successfully applied and quantified in pulmonary volume research during the breathing cycle (12). Additionally, the introduced technique was applied in patients with intra- (solitary intrapulmonary) and extrapulmonary (malignant pleural mesothelioma) malignancies to evaluate the potential to detect differences or changes in local and global intraparenchymal pulmonary motion.

MATERIALS AND METHODS

Prior to enrolment, the investigation protocol was approved by the institutional human research ethic committee. Twenty-five healthy young non-smoking volunteers (18 male and 7 female; median age, 28 years; range 22 – 33 years) and five healthy elderly non-smoking volunteers (3 male and 2 female; median age, 61 years; range 58 – 62 years) without any evidence or history of pulmonary disease, were included in this study. In addition, five patients (3 male and 2 female; median age, 63 years, range 60 – 65 years) with a histologically proven intrathoracic solitary stage I non-small cell lung cancer (NSCLC) were included in this study (maximum axial diameter 3.5 $\pm$ 1.6 cm; localization: upper lung part: 3, middle lung part: 2 [4, 13]). No therapeutical treatment had been performed before the MRI examination. Stage I patients were chosen to guarantee certain intrathoracic restrictions in pulmonary motion.

Lastly, five patients with a histologically proven stage II malignant pleural mesothelioma (MPM; 3 male and 2 female; median age, 60 years; range 58 – 63 years) were included in this study (stage II = T2 N0 M0 = tumor involves any of the ipsilateral pleural surface with at least one of the following: confluent visceral pleural tumor (including fissure), invasion of diaphragmatic muscle, invasion of lung parenchyma. Stage II patients were chosen to guarantee certain extrathoracic restrictions in pulmonary mobility. Upon histological verification of the tumor, we determined that no treatment had been performed before chemotherapy (CHT; combination of pemetrexed and cisplatin [14]). Patients were investigated before CHT and after three out of six cycles (9 weeks).

After the nature of the procedure had been fully explained, informed consent was signed by all participants under an institutionally approved subject research protocol.

MRI

All examinations were performed using a clinical 1.5T whole-body scanner (Magnetom Symphony, Siemens Medical Solutions, Erlangen, Germany) equipped with eight receiver channels, a six channel coil and a high performance gradient system (30 mT/m) (8, 9).

For lung motion examination dynamic breathing MRI were performed as follows (Fig. 1):

3D+t (dynamic 3D-MRI = 3D-MRI during the breathing cycle [9, 12]).

An MRI was performed using an isotropic time-resolved 3D gradient echo pulse sequence. In this study, the view sharing methods used, have been proven to be suitable in the investigation of the lung and lung tumor motion (8–10, 15). In this technique some parts of k-space are updated more often than other k-spaces, leading to an effective shortening of the total acquisition time. For 3D-applications, the view sharing implementation, time-resolved interpolated contrast kinetics (TRICKS), was introduced (15) and applied as per the manufacturer's instructions (SIEMENS). In TRICKS, the low frequency k-space data which contributes most significantly to the image content is sampled more frequently than the high frequency k-space data which is interpolated between consecutive time frames (FLASH [fast low angle shot] 3D; TR/TE = [repetition time/echo time]: 1.54/0.59 msec, flip angle = 10°, receiver bandwidth = 1,500 Hz/pixel; GRAPPA acceleration factor = 3, FOV [field of view]: 375 × 400 mm, matrix = 77 × 128, slab thickness = 198 mm, 52 partitions, voxel size = 4.87 × 3.13 × 3.8 mm^3). Consecutive data sets were acquired over 20 seconds during the following breathing

maneuver: All volunteers were instructed to maximally exhale before the start of the measurement and to slowly breathe in to maximum inspiration (within 5 seconds) during the measurement and, once again, to exhale slowly. Thus, MRI measurements started at the maximum expiratory level and covered continuous maximum inspiration and maximum expiration. A slow breathing maneuver was performed to account for the low temporal resolution of one 3D dataset per second. This procedure was rehearsed several times to ensure a reproducible execution. All subjects were instructed to breathe uniformly for the MRI.

2D-Dynamic MRI

In recent studies, it has been shown that there are significant correlations between 3D- and 2D-dynamic MRI techniques (8, 14). A 2D-MRI technique was used for comparison with the introduced 3D-MRI technique because of the better temporal resolution and the less time-consuming quantification process. For a 2D-dynamic MRI, a fast imaging with a steady precession (trueFISP) pulse sequence using the following applied imaging parameters (4): TE/TR = 1.7/37.3 ms, flip angle 65°, receiver bandwidth 977 Hz pixel 21, GRAPPA acceleration factor = 2, reference k-space lines for calibration 31, FOV = 375 × 400 mm, matrix 112 × 192, slice thickness 10 mm. View sharing was not used for the 2D-method. Three frames per second (scan time per frame is 0.33 s) were acquired within an acquisition time of 30 s. All patients were instructed to change from quiet tidal breathing to maximal inspiration and maximal expiration, as in 3D- imaging.

Analysis

Quantification of lung motion

While 2D+t MRI image sequences offer enough detail from the intraparenchymal region for image based non-rigid registration, 3D+t image sequences suffer from a low signal-to-noise ratio and virtually no morphological information from within the lungs (8, 9, 14). Thus, when applying non-rigid registration methods to 3D+t image sequences acquired as described above, the calculated motion information does not necessarily correspond to the real motion of the parenchyma. Depending on the degree of regularization applied during the algorithmic solution of the registration problem, it represents either an interpolation of the motion observed at areas with reliable image information (mostly outside of the lung), or a quantification of the motion of local image noise.

Thus, we have elaborated an alternative approach for the approximation of local parenchymal motion during the respiratory cycle by the interpolation of a dense vector field from a set of points residing on the surface of the lung. These point set correspondences are established automatically by means of a statistical shape model. In the following, it will be briefly summarized as to which steps are performed in the estimation of motion information from a set of consecutive 3D-images.

In medical image processing, a statistical shape model may be used to solve the problem of segmentation in cases where the desired object has a reasonably known shape. While for a human being it is straightforward to recognize the three-dimensional shape of an object, it is a challenging

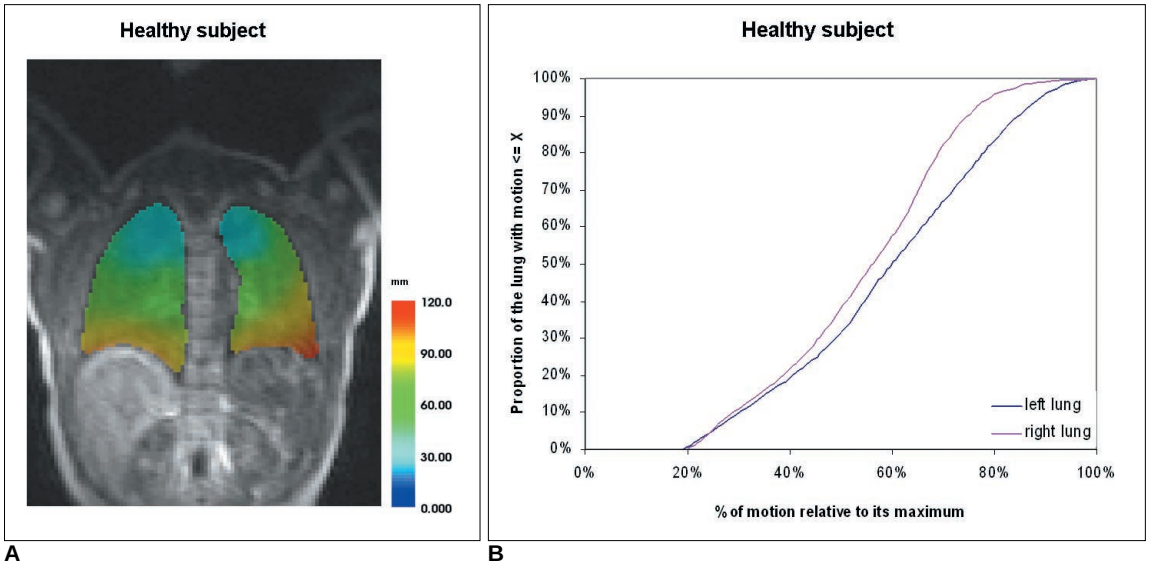

A B

Fig. 1. Motion information of healthy subject covering whole breathing cycle.
A. Color map shows absolute strength of motion (maximum extension from end-inspiration to end-expiration). Upon comparison, it can clearly be seen that most substantial symmetric intraparenchymal motion is in lower parts of lung.
B. Cumulative motion histogram shows relative motion of lung to its maximum.

task to represent shape information in a way that a computer understands. Therefore, the principle of statistical shape modeling has been introduced (16). Given a set of training shapes where each shape in the training set is represented by a set of labeled landmark points which must be consistent from one shape to the next, a statistical shape model is calculated. Such a model consists of the mean shape across all training shapes, combined with the associated variance information. Additionally, this shape information may be combined with information about the gray-value appearance of each of the training shapes. This way, segmenting the desired object in new image data corresponds to finding model parameters which minimize the difference between the image and a synthesized model example, projected into the image. The segmentation result is typically represented as a mesh where each vertex corresponds to one of the labelled landmark points. By applying such a shape-based segmentation method to a temporal series of consecutive images, one gains anatomic correspondence information, because corresponding vertices in the segmentation result should approximately be located at the same anatomic positions.

The shape-based segmentation approach used in this work is based on the work of Heimann et al. (17), who combined the shape information from a statistical shape model with a locally deformable model. This extends the applicability of the segmentation method to a broader range of data sets, including shape variations that have not been observed in the set of training shapes. Using the methods described by Heimann et al. (18), we have built statistical shape models of the left and right lung from 180 lung segmentations in all includes subjects. Each shape model consists of a set of 1,000 points. As a certain gold standard maximum motion of the basal lung parts, using an established quantitative 2D-MRI-technique, was applied (4) and compared with the introduced technique. The whole training dataset has been segmented by a radiological expert.

The workflow for calculating dense vector fields from a 3D+t image sequence has been implemented in an interactive software environment based on our open-source toolkit for interactive medical image processing applications, MITK (Medical Imaging Interaction Toolkit) (19). There, the following steps have to be performed: First, a 3D-surface model representing the mean model of the lung is positioned roughly within the first data set of the time series. Then, the shape-based segmentation algorithm automatically segments the lung within that dataset. The segmentation result may be verified and corrected if necessary. Then, this initial segmentation is propagated automatically to all other time steps of the image sequence by applying the segmentation result of the previous time step as initialization of the shape model in the current time step. As a result of the segmentation process, a series of corresponding points (1,000 for every time step) is generated. This correspondence information gives detailed information about the motion of the lung surface. A dense vector field representing the motion from one time step to the next may be calculated by initializing an elastic body spline transformation (EBS-transform) with correspondence information from the landmarks. An EBS-transform maps a set of landmark locations in one image onto a corresponding set on a second image-based on the theory of deformable bodies. For a time series of N images, a set of N-1 vector fields is calculated, revealing detailed information about the local motion of the lung.

Data Analysis

To facilitate an intuitive way of interpretation for the vector fields, motion information is coded into a color map by accumulating all the motion information onto the first time step of the image sequence. The motion of each single voxel within the lung is tracked over time and the total distance (end inspiration to end expiration as for the 2D-technique) that is covered by this voxel is color coded. The absolute motion of the voxel and lung parenchyma is shown. The color maps are rendered as transparent overlays onto the original images. Additionally, the vector fields can be displayed explicitly in a three-dimensional view by arrow representations.

When the data of one patient should be assessed in follow-up examinations or in a comparison of the hemithoraces, it is hard to compare motion information because intra-individual differences of the magnitude of the breathing maneuver cannot be distinguished from potential changes due to treatment response. Normally, there is no substantial difference between the hemithoraces in healthy subjects. Thus, we propose an alternative strategy by expressing the strength of the motion in the diseased hemithorax, relative to the strength of motion in the healthy hemithorax. Additionally, motion information is normalized to its relative strength. This way, the individual motion pattern can be displayed in a cumulative histogram, which relates the relative strength of the motion to the proportion of the lung in which motion, smaller or equal to the given strength, can be observed.

To get an impression of what can be regarded as a 'normal' non-pathologic motion pattern, a mean cumulative motion histogram has been calculated.

In this proof-of-principle study, a group of healthy volunteers was investigated and color maps and cumulative motion histograms were performed. Results were

compared with a patient with NSCLC and with a patient with MPM.

For 2D-dynamic MRI lung motion examination, coronal planes crossing the trachea were acquired in each patient (4). Motion of the lung was measured from the apex of the lung to the diaphragmatic dome in the craniocaudal (CC) plane in the middle of the hemithorax. Maximum displacement was defined as the maximum difference between deep inspiration and expiration using MRI.

Statistical Analysis

Statistical analyses were performed using the SAS software (SAS Institute Inc., Cary, NC). To obtain simultaneous tests for the mean comparisons, the Duncan's multiple-range test of analysis of variance on the significance level of $p = 0.05$ was used. The mean and standard deviation were calculated. In addition, a *t*-test performed on paired samples was performed. Further, a correlation of the 2D- dynamic MRI data with 3D-dynamic MRI data was investigated by a Spearman's correlation. For the correlation maximum, craniocaudal motion of the basal lung parts was measured using a 2D-dynamic MRI (4) and a 3D-dynamic MRI and was tested to determine whether a correlation between the two modalities was evident. Voxel motion was defined as the maximum motion of a voxel (mm) during respiration. Statistical significance was set at $p < 0.05$.

RESULTS

In all healthy subjects, information on local and global lung parenchymal motion could be visualized and estimated (color map, Fig. 1A). Maximum lung motion (motion of the voxel that moves greatest distance) in the basal lung parts was about 9.2 $\pm$ 3.1 cm and no significant difference between both hemithoraces was found. The associated motion trajectory was calculated over each voxel and then visualized. A relative cumulative motion histogram showed the same information (Fig. 1B). Using the 2D-dynamic MRI technique, maximum CC motion was determined to be 8.8 $\pm$ 3.5 cm, which represented no significant difference between the hemithoraces. A correla-

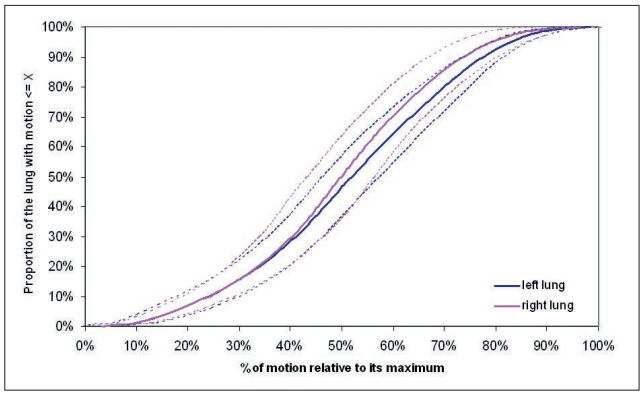

Fig. 2. Mean cumulative relative motion histogram calculated over 30 healthy volunteers. Dotted lines indicate corresponding standard deviations.

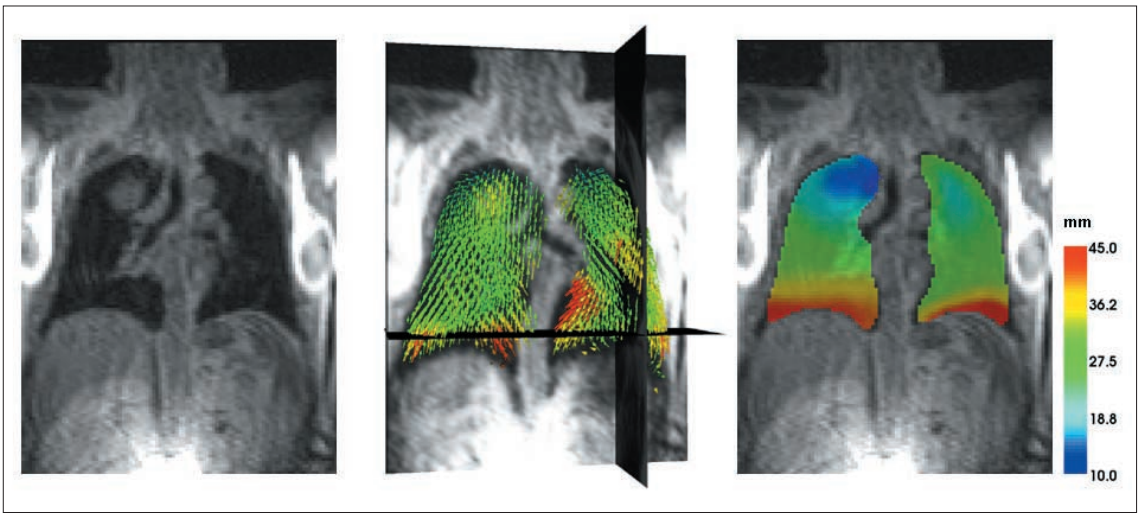

Fig. 3. MRI depiction of parenchymal lung motion.
A. Patient with solitary non-small cell lung cancer in upper right lung.
B. Using simple vector field representation for one time frame of breathing cycle, limited lung motion in right upper lung can hardly be seen.
C. Using color map representation of breathing cycle, from maximum expiration to maximum inspiration, limited asymmetric lung motion can clearly be seen. In this patient, overall lung motion was limited because of limited lung function.

tion between the 3D- and 2D-MRI measurement of maximum motion in the basal lung parts was found to be significant ($r = 0.89$, $p < 0.05$, Table 1).

Motion Model

The mean cumulative relative motion histogram and standard deviations, calculated from 30 healthy volunteers, is shown in Figure 2. In healthy persons, similar motion patterns can be expected for the left and right lungs. An analysis comparing younger to older healthy individuals indicated no significant difference ($p = 0.31$).

Patient with Non-Small Cell Lung Cancer

Cumulative vectorial and color maps are not shown in the group of patients because of the different localizations of the tumors and thus different influences on the intraparenchymal lung motion at different localizations. In Table 1, maximum craniocaudal motions of the basal lung parts are shown. Intraparenchymal lung motion during respiration is shown using vectorial and color map techniques (Fig. 3). A substantial restriction of the lung motion around the tumor can be observed.

Patient with Malignant Pleural Mesothelioma

Intraparenchymal lung motion during respiration is shown using the color map technique, before and after therapy (Fig. 4). A substantial restriction of the whole intraparenchymal lung motion in comparison with healthy volunteers (Fig. 1), is shown. A slight improvement of lung mobility can be observed after therapy. In Table 1,

Table 1. Maximum Motion of Basal Lung Parts

Maximum Motion of Basal Lung Parts (cm)	2D-Dynamic MRI	3D-Dynamic MRI Using Color Maps
Healthy volunteer	8.8 ± 3.5	9.2 ± 3.1
Patient with a solitary NSCLC		
- healthy hemithorax	8.5 ± 3.1	8.2 ± 3.4
- hemithorax with NSCLC	7.8 ± 3.5	7.5 ± 3.1
Patient with MPM, before CHT		
- healthy hemithorax	8.8 ± 3.1	9.1 ± 2.9
- hemithorax with MPM	2.6 ± 1.0*	2.5 ± 1.1*
Patient with MPM, after CHT		
- healthy hemithorax	8.9 ± 2.9	8.9 ± 2.8
- hemithorax with MPM	4.3 ± 1.6*	4.5 ± 1.5*

Note.— As there was no significant level of maximum motion of basal lung parts in healthy volunteers, there is only one value. In patients with solitary non-small cell lung carcinoma and patients with malignant pleural mesothelioma before and after chemotherapy, hemithorax is subdivided based on presence of tumor or not. Follow-up of patients with malignant pleural mesothelioma indicated significant improvement in maximum motion of basal lung parts of hemithorax with malignant pleural mesothelioma, which could be proven using 2D- and 3D-techniques, as well as in end volumetry. Correlation between 2D- and 3D-dynamic MRI using color maps was significant in all cases ($p < 0.01$).
(* significant change [$p < 0.01$], 2D-dynamic MRI $p = 0.009$, 3D-dynamic MRI $p = 0.08$)
NSCLC = non-small cell lung carcinoma, MPM = malignant pleural mesothelioma, CHT = chemotherapy

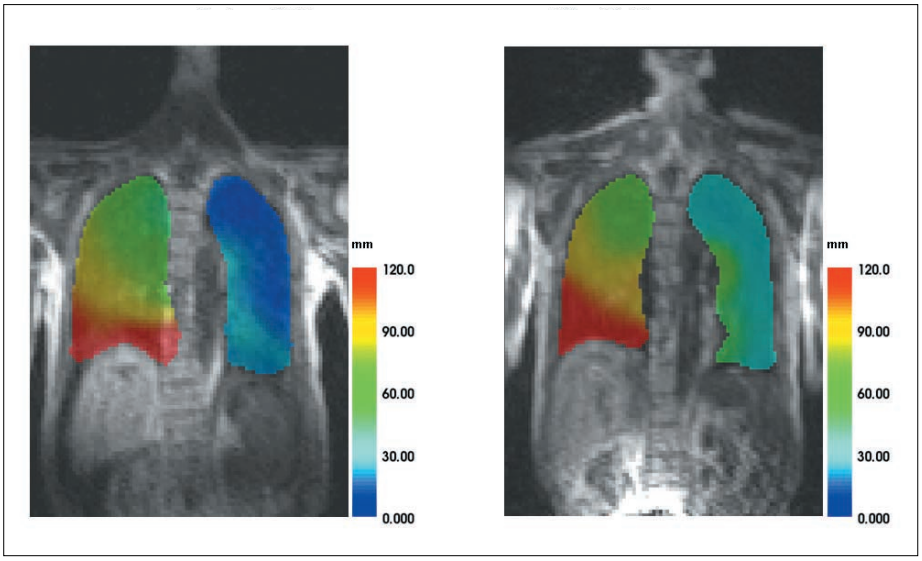

Fig. 4. Patient with malignant pleural mesothelioma in left hemithorax before (left) and after (right) chemotherapy. Substantial restriction of left-sided intrapulmonary motion can be observed. After therapy, lung motion increased slightly and in good correlation with improved lung function.

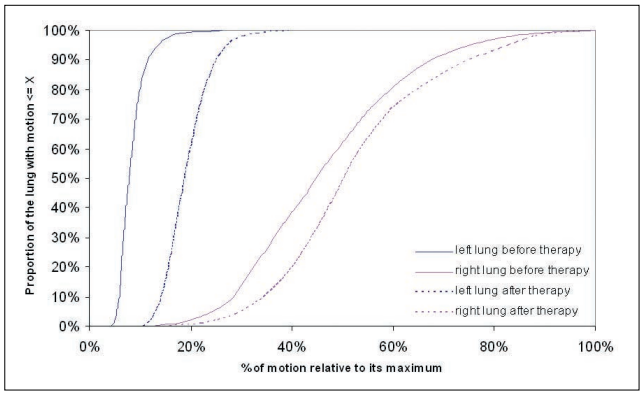

Fig. 5. Cumulative relative motion histogram for patient with malignant pleural mesothelioma (from Fig. 4). Following therapy, slight increase of overall lung motion, especially left side, can be observed.

absolute data concerning the maximum CC motion indicate a significant improvement of the motion of the MPM-bearing hemithorax. This improvement was also found by clinically performed pulmonary function tests (vital capacity 2.9 $\pm$ 0.5 versus 3.4 $\pm$ 0.6 L, FEV1 0.9 $\pm$ 0.2 versus 1.4 $\pm$ 0.2 L), but was not proven to be significant.

The cumulative relative motion histogram for the same patient (Fig. 5), indicates a decrease in lung motion in the left lung before therapy is apparent. The increase in lung mobility after therapy is demonstrated as a shift of the motion curves to the right.

DISCUSSION

The results of this study indicate that a dynamic 3D-MRI, using a parallel imaging technique in combination with an introduced post-processing technique, is able to quantify intraparenchymal lung motion during the breathing-cycle in healthy volunteers and patients with intra- and extrapulmonary tumors. According to recent studies significant correlations between 2D- and 3D-imaging techniques could be proven (12); however, these studies have focused only on extrapulmonary structures (e.g. the thorax and the diaphragm). In this study, the measurement of intraparenchymal dimensions indicated a significant correlation between 2D- and 3D-techniques. The established 2D-technique (4, 5), which measures the motion of extrapulmonary landmarks, was applied and proven to show significant correlations with the proposed 3D-technique by accurately measuring intraparenchymal lung motions, especially of the basal lung parts. It might be argued that both techniques measured two different aspects and thus were not comparable. However so, it is only to a certain degree. The 2D-technique measured absolute dimensions (e.g. maximum extension from in- to expiration using extrapulmonary landmarks), as did the 3D-technique, but did so using intraparenchymal voxels. Both techniques showed similar measurements, which was verified in the basal lung parts. In summary, both absolute quantifications showed a significant correlation and the established 2D-technique proved to be a suitable and simple technique to check and prove the validity of the 3D-technique. Using the 3D-technique, significant local and global intraparenchymal pulmonary differences during the breathing cycle could be demonstrated, which might be of interest in future research e.g. in the field of therapy monitoring or follow-up investigations of pulmonary diseases. Using global lung function tests (in this case: spirometry in patients with MPM), substantial changes in lung function could be quantified. However, due to the inherent deficit to quantify local changes, these changes were not significant compared with local MRI-techniques.

It might be argued that the authors focused on malignant intra- and extrapulmonary tumors to investigate the introduced technique measuring motion of the lung. The reasoning behind this decision was attributed to the authors intentions to investigate the introduced technique in two established lung disease models, where an influence on lung motion using MRI has already been proven in the past (13, 20). The extension of this technique, even on benign pulmonary diseases, might be of interest in further research.

Many approaches exist, when it comes to quantifying lung motion, especially in radiotherapy. These approaches generally focus on the quantification of the changes of extrapulmonary structures, such as the thoracic wall or the diaphragm. One frequent approach is to use fluoroscopy (21); but, as a projection technique, it is very imprecise and lung parenchyma can hardly be visualized. CT has also been proposed in this field (10, 22), but has the inherent limitation of radiation exposure (23). The recent development of fast dynamic MRI techniques has made possible, detailed, non-invasive imaging of pulmonary parenchyma by overcoming the inherent difficulties associated with lung imaging, including low proton density, severe magnetic field susceptibility, and respiratory and cardiac motion artifacts. Thus, MRI has been described as a tool used to quantify lung and tumor motion during respiration (9, 24). It could be shown that MRI is able to encompass the whole thorax and to directly assess impaired respiratory mechanics without using X-rays; an important aspect, especially in follow-up examinations and benign diseases. Gee et al. (11) introduced the 2D-MRI to quantify regional lung strain. It could be demonstrated that knowledge of lung motion is a new way to quantify lung mechanics and

thus regional lung function. Thus far, 3D-techniques have not been investigated.

As observed by Sarrut et al. (10) and Remouchamps et al. (25), using CT, there were lower parenchymal displacements in the upper lung regions than in the lower parts. In contrast to a CT, where standardized Hounsfield units can be used to support the segmentation process, automatic MRI-based segmentation is a more challenging task. Recent developments in the area of shape-based segmentation have helped to overcome these problems, thus facilitating a fully automatic segmentation of the lungs, even in noisy data. As an inherent property of all shape-based segmentation methods, shape correspondence can be established either between the shape model and the image by segmenting the image or even between two images by the segmentation of both images using the same shape model. This opens a wide field for image analysis requiring correspondence information, as is the case for motion estimation. However, there are also several aspects of this method which have to be discussed. On the one hand, the main limitation is that motion information is estimated by interpolating internal motion from motion at the surface of the lung. On the other hand, having no further information available about the internal structure of the lung parenchyma, this is a reasonable approach as a first step towards establishing applicability of elastic body splines and 3D+t motion information at all. If internal structures are clearly visible in all time steps using enhanced image sequences, the method could easily be extended to add these internal landmarks to the set of corresponding landmarks. This way, local internal parenchymal motion could also be modeled. The presented method represents a novel, semi-automated way to evaluate lung motion in three dimensions over time. This was proven in a series of healthy subjects. For verification, we used an established 2D-MRI technique. Also significant correlation was found between the 2D- and 3D-methods and the results were similar to recent results, verified by spirometry (4).

In the next step we investigated whether the technique is able to show changes of intraparenchymal lung motion in patients with intra- and extrapulmonary tumors. Recently, it has been shown that intrapulmonary tumors have a significant influence on lung motion of the tumor bearing hemithorax (9). In this study it has been proposed that regional disorders of the lung motion by lung tumors might be a reason for the disorder of the lung compliance. Comparing tumor bearing with the non-tumor bearing hemithorax supports this observation; especially in the area around the tumor where a substantial decrease in lung motion could be observed. This decrease might be caused by the infiltrative and retractive effects of the tumor, and requires further research.

In patients with extrapulmonary tumors (e.g. pleural mesothelioma), restriction of the mobility of the tumor bearing the hemithorax can be expected (26). In this study, we could show that an extrapulmonary tumor mass leads to a substantial global decrease in lung mobility and thus intraparenchymal motion. Additionally, it could be proven that significant changes of this decrease in intraparenchymal lung mobility after CHT can be shown using the proposed MRI technique, and verified by spirometry.

Still, a major limitation in using 3D-MRI techniques is the limited temporal resolution of one image per second. The investigator is hardly dependent on the good breathing compliance of the patient. Even though this temporal resolution proved to be suitable in the past research of patients with pulmonary diseases (9, 12), an improvement in the temporal as well as the spatial resolution must be recommended to better cover a whole breathing cycle, especially in tidal breathing.

If this new technique is sensitive enough to examine slight changes during a follow-up examination of a bigger group of patients, it might have the potential to be an early predictor of therapy response, however this needs to be proven in further research. Also the potential to assist in the detection of early, localized, and benign pathologies (e.g. fibrotic diseases at a stage not influencing spirometry) has recently been published, however measuring pulmonary volumetric dimensions (27) has to be verified in further research.

In conclusion, the dynamic 3D-MRI in combination with a novel post-processing technique has shown to be a usable 3D-tool for the quantification of intraparenchymal lung motion. This technique is able to show differences between the intraparenchymal lung motion of healthy volunteers and patients with intra- and extrathoracic lung diseases, and thus might have the potential to be a tool to investigate slight changes of local and global pulmonary mechanics.

References

1. Petty TL, Silvers GW, Stanford RE. Mild emphysema is associated with reduced elastic recoil and increased lung size but not with air-flow limitation. *Am Rev Respir Dis* 1987;136:867-871
2. Clausen JL. The diagnosis of emphysema, chronic bronchitis and asthma. *Clin Chest Med* 1990;11:405-416
3. Suga K, Tsukuda T, Awaya H, Takano K, Koike S, Matsunaga N, et al. Impaired respiratory mechanics in pulmonary emphysema: evaluation with dynamic breathing MRI. *J Magn Reson Imaging* 1999;10:510-520
4. Plathow C, Ley S, Fink C, Puderbach M, Heilmann M, Zuna I, et al. Evaluation of chest motion and volumetry during the breathing cycle by dynamic MRI in healthy subjects: comparison with pulmonary function tests. *Invest Radiol* 2004;39:202-209

5. Plathow C, Fink C, Ley S, Puderbach M, Eichinger M, Schmähl A, et al. Measurement of diaphragmatic length during the breathing cycle by dynamic MRI: comparison between healthy adults and patients with an intrathoracic tumor. *Eur Radiol* 2004;14:1392-1399
6. Axel L, Dougherty L. MR imaging of motion with spatial modulation of magnetization. *Radiology* 1989;171:841-845
7. Napadow VJ, Mai V, Bankier A, Gilbert RJ, Edelman R, Chen Q. Determination of regional pulmonary parenchymal strain during normal respiration using spin inversion tagged magnetization MRI. *J Magn Reson Imaging* 2001;13:467-474
8. Fink C, Ley S, Kroeker R, Requardt M, Kauczor HU, Bock M. Time-resolved contrast-enhanced three-dimensional magnetic resonance angiography of the chest: combination of parallel imaging with view sharing (TREAT). *Invest Radiol* 2005;40:40-48
9. Plathow C, Schoebinger M, Fink C, Hof H, Debus J, Meinzer HP, et al. Quantification of lung tumor volume and rotation at 3D dynamic parallel MR imaging with view sharing: preliminary results. *Radiology* 2006;240:537-545
10. Sarrut D, Boldea V, Ayadi M, Badel JN, Ginestet C, Clippe S, et al. Nonrigid registration method to assess reproducibility of breath-holding with ABC in lung cancer. *Int J Radiat Oncol Biol Phys* 2005;61:594-607
11. Gee J, Sundaram T, Hasegawa I, Uematsu H, Hatabu H. Characterization of regional pulmonary mechanics from serial magnetic resonance imaging data. *Acad Radiol* 2003;10:1147-1152
12. Plathow C, Schoebinger M, Fink C, Ley S, Puderbach M, Eichinger M, et al. Evaluation of lung volumetry using dynamic three-dimensional magnetic resonance imaging. *Invest Radiol* 2005;40:173-179
13. Plathow C, Ley S, Fink C, Puderbach M, Hosch W, Schmähl A, et al. Analysis of intrathoracic tumor mobility during the whole breathing cycle by dynamic MRI. *Int J Radiat Oncol Biol Phys* 2004;59:952-959
14. Vogelzang NJ, Rusthoven JJ, Symanowski J, Denham C, Kaukel E, Ruffie P, et al. Phase III study of pemetrexed in combination with cisplatin versus cisplatin alone in patients with malignant pleural mesothelioma. *J Clin Oncol* 2003;21:2636-2644
15. Du J, Bydder M. High-resolution time-resolved contrast-enhanced MR abdominal and pulmonary angiography using a spiral-TRICKS sequence. *Magn Reson Med* 2007;58:631-635
16. Cootes TG, Taylor CJ, Cooper DH, Graham J. Active shape models - their training and application. *Comput Vis Image Underst* 1995;61:38-59
17. Heimann T, Münzing S, Meinzer HP, Wolf I. A shape-guided deformable model with evolutionary algorithm initialization for 3D soft tissue segmentation. *Inf Process Med Imaging* 2007;20:1-12
18. Heimann T, Wolf I, Meinzer HP. Automatic generation of 3D statistical shape models with optimal landmark distributions. *Methods Inf Med* 2007;46:275-281
19. Wolf I, Vetter M, Wegner I, Böttger T, Nolden M, Schöbinger M, et al. The medical imaging interaction toolkit. *Med Image Anal* 2005;9:594-604
20. Plathow C, Klopp M, Schoebinger M, Thieke C, Fink C, Puderbach M, et al. Monitoring of lung motion in patients with malignant pleural mesothelioma using two-dimensional and three-dimensional dynamic magnetic resonance imaging: comparison with spirometry. *Invest Radiol* 2006;41:443-448
21. Hof H, Herfarth KK, Münter M, Hoess A, Motsch J, Wannenmacher M, et al. Stereotactic single-dose radiotherapy of stage I non-small-cell lung cancer (NSCLC). *Int J Radiat Oncol Biol Phys* 2003;56:335-341
22. Hof H, Herfarth KK, Münter M, Essig M, Wannenmacher M, Debus J. The use of the multislice CT for the determination of respiratory lung tumor movement in stereotactic single-dose irradiation. *Strahlenther Onkol* 2003;179:542-547
23. Shirato H, Oita M, Fujita K, Watanabe Y, Miyasaka K. Feasibility of synchronization of real-time tumor-tracking radiotherapy and intensity-modulated radiotherapy from viewpoint of excessive dose from fluoroscopy. *Int J Radiat Oncol Biol Phys* 2004;60:335-341
24. Plathow C, Fink C, Ley S, Puderbach M, Eichinger M, Zuna I, et al. Measurement of tumor diameter-dependent mobility of lung tumors by dynamic MRI. *Radiother Oncol* 2004;73:349-354
25. Remouchamps VM, Letts N, Yan D, Vicini FA, Moreau M, Zielinski JA, et al. Three-dimensional evaluation of intra- and interfraction immobilization of lung and chest wall using active breathing control: a reproducibility study with breast cancer patients. *Int J Radiat Oncol Biol Phys* 2003;57:968-978
26. Eibel R, Tuengerthal S, Schoenberg SO. The role of new imaging techniques in diagnosis and staging of malignant pleural mesothelioma. *Curr Opin Oncol* 2003;15:131-138
27. Plathow C, Hof H, Kuhn S, Puderbach M, Ley S, Biederer J, et al. Therapy monitoring using dynamic MRI: analysis of lung motion and intrathoracic tumor mobility before and after radiotherapy. *Eur Radiol* 2006;16:1942-1950